Journal of Japan Association for Earthquake Engineering, Vol. 20, No. 8, 2020

# VARIATION IN SOURCE CHARACTERISTICS OF REPEATING M6-CLASS PLATE-BOUNDARY EARTHQUAKES OFF KESENNUMA, NORTHEAST JAPAN

Kimiyuki ASANO[1]

[1] Member, Associate Professor, Disaster Prevention Research Institute, Kyoto University, Uji, Japan, k-asano@egmdpri01.dpri.kyoto-u.ac.jp

**ABSTRACT**: Nowadays, the scenario-based strong motion prediction is strongly required quantitatively to show its diversity and uncertainty. We focus on the variation or uncertainty in source parameters such as the size and stress drop of the strong motion generation area (SMGA). Repeating M6-class plate-boundary earthquakes occurring off Kesennuma, northeast Japan, were analyzed. The latest event on May 13, 2015 ($M_{JMA}$ 6.8) had two SMGAs, and each event in 1973, 1986 and 2002 had one SMGA. The SMGA1 of the 2015 event and SMGAs of the other three events were close to each other in space, and their spatial extent was almost same. The variation in the estimated stress drop of SMGA was approximately less than 1.6 times of the smallest event.

**Keywords**: Repeating earthquake, Plate-boundary earthquake, Strong motion generation area, Stress drop

## 1. INTRODUCTION

The lesson from the 2011 Tohoku earthquake made the earthquake engineering and seismological communities be more and more aware of the diversity and uncertainty in the scenario-based strong motion prediction[1]. This paper particularly focuses on the source parameters among the factors that cause variation and uncertainty in the strong motion prediction. The spatial size and stress drop of the source fault and strong motion generation area (SMGA) can be given according to some empirical source scaling relationships in the framework of the recipe for strong motion prediction from a specific source fault[2, 3]. These empirical source scaling relationships were developed based on source models analyzed for past earthquakes[4], and each earthquake in the original data set has its own deviation from the average scaling relationship. This deviation includes two sources of variation. One originates in the tectonic differences of each source region. The other is aleatory uncertainty as the nature of earthquakes itself, which reflects variation in source parameters among earthquakes occurring in a specific source region. There are many literatures studying the source scaling relationships for small-to-moderate earthquakes in the world, and these studies show no significant variation in stress drops with seismic moment, which implies earthquake self-similarity, but stress drop estimates for the analyzed earthquakes have large variation over two to three orders of magnitude[5, 6]. However, variation in source parameters among large earthquakes occurring in one and the same source region is not resolved well. Knowledge on the true variations or uncertainties inherent in the earthquake phenomenon itself would lead us to use rational probability distributions of source parameters in strong motion prediction.

Studying repeating earthquakes occurring in an identical source region would contribute to responding to this request. One of the pioneering studies is the asperity map for the subduction-zone plate-boundary earthquakes along the Japan Trench[7), 8)]. From the viewpoint of strong motion prediction, it is especially important to accumulate knowledge about which source parameter of SMGA is invariant and which is not. Repeating moderate-to-large earthquakes in northeastern Japan have been recorded two or more times in the history of strong motion observation. For example, Takiguchi et al.[9)] modeled the source processes of two $M_{\mathrm{JMA}}$ 7.0 earthquakes in 1982 and 2008 occurring on the plate-boundary offshore of Ibaraki Prefecture, Kanto, Japan. They reported that there were clear differences in the foreshock activities, initial rupture processes, and the locations of the rupture starting point between the 1982 and 2008 mainshocks. Nevertheless, each $M_{\mathrm{JMA}}$ 7.0 event had a SMGA rupturing in a similar way at almost the same location with the spatial extent equivalent to each other, but the 1982 event had 1.5 times larger stress drop in the SMGA than the 2008 event.

This paper analyzed M6-class repeating earthquakes occurring on the plate-boundary offshore of Kesennuma, northeast Japan, whose average recurrence interval was about 15 years. The last two events in November 2002 and May 2015 were densely observed by the nation-wide strong motion networks K-NET and KiK-net of the National Research Institute for Earth Science and Disaster Resilience (NIED). The Strong-Motion Earthquake Observation Network in Japanese Ports with a history of more than half a century[10)] has recorded strong ground motions at the same location from the last four events. The variation in the source parameters among the last four off-Kesennuma earthquakes will be discussed based on the strong motion waveform modeling using the empirical Green's function method[11)].

## 2. REPEATING PLATE-BOUNDARY EARTHQUAKES OFF KESENNUMA, NORTHEAST JAPAN

According to Hasegawa et al.[12)] and Takasai et al.[13)] who investigated moderate-size repeating earthquakes occurring along the subduction-zone in northeast Japan based on the historical seismograms of the Japan Meteorological Agency (JMA), M6-class earthquakes have occurred repeatedly on the plate-boundary interface off Kesennuma (Table 1 and Fig. 1). It was reported that the average recurrence interval was 15.5 years and the average $M_{\mathrm{JMA}}$ was 6.3. Then, another earthquake of $M_{\mathrm{JMA}}$ 6.8 occurred on May 13, 2015, about 12.5 years after the previous earthquake on November 3, 2002. As shown in Table 1, the earthquake magnitude was different for each event, and the 2015 event was the largest among the last six events. The seismic moment of the moment-tensor solution by the NIED F-net project was estimated to be $1.71\times10^{19}$ Nm for the 2015 off-Kesennuma earthquake, which was 4.4 times larger than the seismic moment ($3.87\times10^{18}$ Nm) of the 2002 off-Kesennuma earthquake. This fact infers that there are clear variations in the source characteristics of each earthquake.

A SMAC-B2 strong motion accelerograph was installed in October 1968 at the Ofunato-bochi strong motion station (OFN) located near the tsunami breakwater in Ofunato Port, Iwate Prefecture, as a part of the Strong-Motion Earthquake Observation Network in Japanese Ports[14)]. The instrument was replaced by an ERS-G digital accelerograph in August 1997, and it was updated again to the Omni type accelerograph in 2013. This strong motion station was constructed on an outcrop of slate rock. The online database of the Strong-Motion Earthquake Observation Network in Japanese Ports operated by the Ministry of Land, Infrastructure, Transport and Tourism (MLIT) and Port and Airport Research Institute (PARI) also provides the waveform records processed into SMAC-equivalent records for the digital records after the update of strong-motion seismographs so that they can be compared with past analog records. Figure 1 shows a comparison of the velocity waveforms in 0.2–2 Hz of the east-west components of the SMAC or SMAC-equivalent records at OFN during the last four events. The peak amplitude of the S-wave portion was largest during the 2015 event. The amplitudes of the 1986 and 2002 events were about the same, and the 1973 event was larger than the 1986 and 2002 events, but much smaller than the 2015 event. However, the four records had almost the same pulse width (about 0.8 s) when we compared the waveforms normalized by the peak amplitude of the first pulse in each waveform (bottom right plot in Fig. 1). It infers that the rupture duration of the major SMGA was almost the same for these four events. Thus, if SMGAs of almost the same area were ruptured during these events, the difference in the stress drop was reflected in the amplitudes of the observed ground motions.

Table 1 Hypocenter information of repeating earthquakes off-Kesennuma by JMA

| Origin Time (JST) | Latitude | Longitude | Depth (km) | $M_{JMA}$ |
|---|---|---|---|---|
| 1940/11/20 00:01 | 38°50.35'N (1.57') | 142°10.93'E (3.98') | 41 | 6.6 |
| 1954/11/19 05:44 | 38°54.26'N (1.60') | 142°06.56'E (4.36') | 52 | 6.1 |
| 1973/11/19 22:01 | 38°51.77'N (1.29') | 142°05.98'E (3.25') | 46.48 (4.66) | 6.3 |
| 1986/12/01 05:15 | 38°52.5'N (0.5') | 142°00.82'E (1.3') | 50.8 (2.0) | 6.0 |
| 2002/11/03 12:37 | 38°53.79'N (0.27') | 142°08.32'E (0.58') | 45.81 (0.93) | 6.3 |
| 2015/05/13 06:12 | 38°51.77'N (0.25') | 142°09.01'E (0.56') | 46.24 (0.92) | 6.8 |

* Values in parentheses indicate the standard errors of hypocenter locations in the JMA catalog.

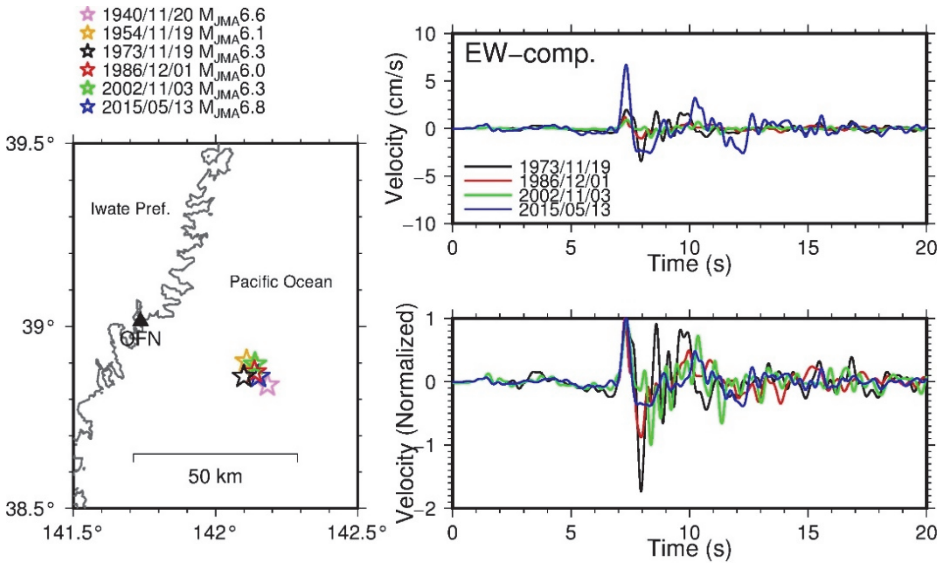


Fig. 1 Map of epicenters and observed velocity waveforms at the Ofunato-bochi station (OFN)

## 3. SOURCE MODELS OF THE 2002 AND 2015 OFF KESENNUMA EARTHQUAKES

### 3.1 Source model of the 2002 off-Kesennuma earthquake

A SMGA source model of the 2002 off-Kesennuma earthquake has been estimated by Suzuki and Iwata[15]. They estimated the source model based on the waveform modeling in 0.4–10 Hz at four K-NET and KiK-net strong motion stations using the empirical Green's function method[11), 16)]. In this study, the SMGA of the 2002 event was reanalyzed using the waveform data from 13 K-NET and KiK-net stations in Iwate and Miyagi Prefectures, northeast Japan. The aftershock records of $M_{JMA}$ 4.8 occurring at 4:14 on November 4, 2002, which was the same event used in Suzuki and Iwata[15], was used as the empirical Green's functions (EGF). As shown in Fig. 2, the focal mechanism of this EGF event analyzed by the NIED F-net project was similar to that of the target event.

First, the parameters $N$ and $C$ necessary for the waveform modeling using the empirical Green's function method were determined by the source spectral ratio function (SSRF) fitting method[16] using the amplitude Fourier spectral ratios between the target and EGF events at 13 stations. Here, $N$ gives the ratio of the source dimensions between the target and EGF events. $C$ is the ratio of the stress drops. In the empirical Green's function method[11, 16], the length, rise time, and seismic moment of SMGA are modeled according to the equations listed in Table 2, which are based on the self-similar source scaling and $\omega^{-2}$ source spectral model. The attenuation factor $Q(f) = 110 f^{0.69}$ by Satoh et al.[18] was used to correct propagation path effects when obtaining the source spectral ratio. As a result, $N$ and $C$ were determined to be 5 and 2.5, respectively.

The techniques for waveform modeling and estimating source parameters using the empirical Green's function method were the same as in the previous study. The SMGA was assumed to be square, and the strike and dip of the source fault plane were set to 184° and 15°, respectively, by referring to the moment tensor solution (MT) by the NIED F-net project. The one-dimensional velocity structure model for the ray tracing was the same model as that used in our previous study for the 2011 Tohoku earthquake[19]. The S-wave velocity at the source depth is 4.46 km/s in this model. Since no significant initial rupture phase was identified in the observed records, the rupture starting point in the SMGA was fixed at the hypocenter located by JMA, which is marked with the green star in Fig. 2. The unknown model parameters included the length, rise time, and rupture propagation velocity of the SMGA, and the rupture starting sub-fault number in the SMGA. These unknown model parameters were estimated by grid search minimizing the sum of the residuals of displacement waveforms and acceleration envelopes of two horizontal components[20]. Table 2 summarizes the search range, search interval, and results for grid search. The SMGA of the 2002 event was estimated to be 5.5 km × 5.5 km, and its rupture propagated southwestward in the down-dip direction. These results were consistent with the previous study[15]. The left panel of Fig. 2 shows the estimated source model, and Fig. 3 shows the waveform fits of the two horizontal components of acceleration, velocity, and displacement waveforms. The broadband strong motion waveforms at each station were successfully reproduced by assuming one SMGA.

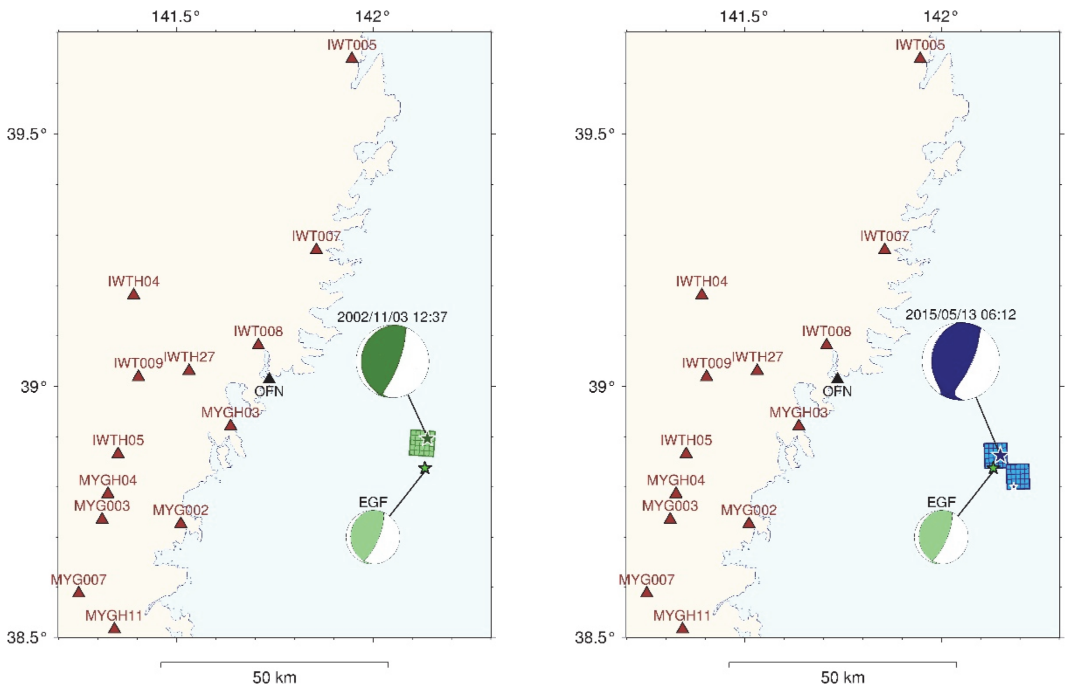


Fig. 2 Source models of the 2002 off-Kesennuma earthquake (left) and the 2015 off-Kesennuma earthquake (right). Green star: The rupture starting point of the 2002 event, Blue stars: The rupture starting point of the 2015 event (large: SMGA1, small: SMGA2), Green yellow star: The epicenter of the EGF event, Triangles: Strong motion stations used in the waveform modeling. Moment tensor solutions by NIED F-net are drawn on the maps using the lower hemisphere projection.

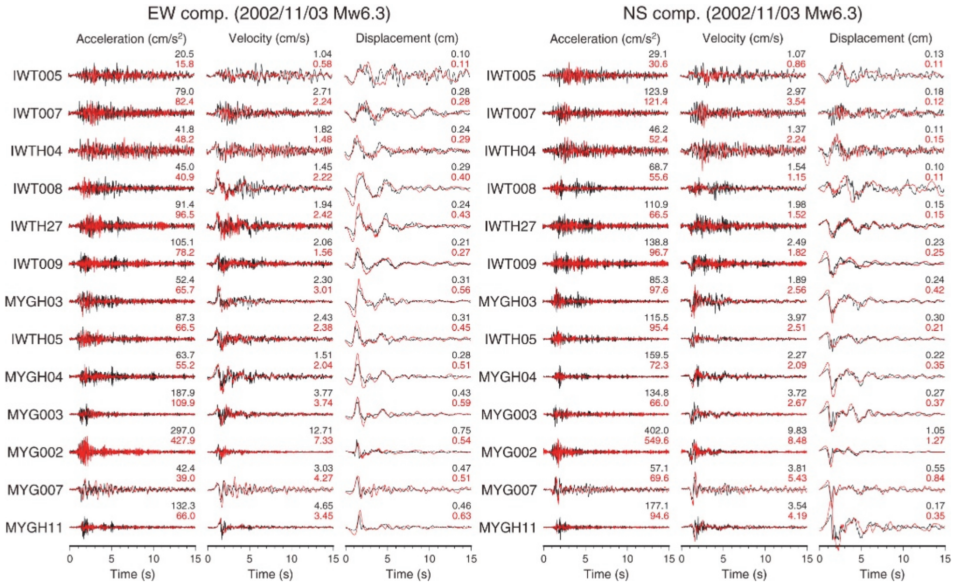


Fig. 3 Observed (black) and synthetic (red) waveforms of the 2002 Kesennuma earthquake. The value above each trace represents the maximum amplitude.

Table 2 SMGA source parameters of the 2002 off-Kesennuma earthquake

| | Parameters | | Search range | Search interval | Results |
|---|---|---|---|---|---|
| EGF | Source dimension $l$ | | 0.3–1.6 km | 0.1 km | 1.1 km |
| | Rise time $\tau$ | | 0.2–0.5 s | 0.02 s | 0.38 s |
| | Seismic moment $m_0$ | | Referring to NIED F-net MT | | $1.31\times10^{16}$ Nm |
| SMGA | Strike / Dip / Rake | | Referring to NIED F-net MT | | 184° / 15° / 74° |
| | $N$ and $C$ | | Estimated by SSRF method | | $N = 5$, $C = 2.5$ |
| | Length $L$ | | $L = N{\cdot}l$ | | 5.5 km |
| | Rise time $T$ | | $T = N{\cdot}\tau$ | | 1.9 s |
| | Rupture velocity | | 2.4–4.0 km/s | 0.2 km/s | 3.6 km/s |
| | Rupture starting point in SMGA | Along strike | 1–5 | 1 | 2 |
| | | Along dip | 1–5 | 1 | 2 |
| | Seismic moment $M_0$ | | $M_0 = CN^3{\cdot}m_0$ | | $4.09\times10^{18}$ Nm |
| | Stress drop $\Delta\sigma$ | | Circular crack model[17)] | | 59.9 MPa |

### 3.2 Source model of the 2015 off-Kesennuma earthquake

Next, the source model of the 2015 off-Kesennuma earthquake was estimated in the same manner. Two distinct wave packets were observed in the strong motion records at many stations. Therefore, a source model consisting of two SMGAs was assumed for this event. The EGF event and strong motion stations used in the waveform modeling were the same as those in the analysis of the 2002 event described in the previous subsection. Since the parameters $N$ and $C$ for two SMGAs cannot be uniquely determined from the source spectral ratio, these parameters were determined by trial and error to better explain the characteristics of the observed waveforms. The source parameters (spatial size and rise time) of the EGF event were the same as the waveform modeling of the 2002 event. Therefore, unknown model parameters were *C* factor, rupture propagation velocity and rupture starting sub-fault of each SMGA, and the rupture time and location of SMGA2 relative to SMGA1, and they were estimated by grid search. Here, it is assumed that two SMGAs were on the same fault plane. The search range, search interval, and results for grid search are summarized in Table 3. The right panel of Fig. 2 shows the estimated source model, and Fig. 4 shows the waveform fits. The stress drops in the two SMGAs were about 1.4–1.6 times larger than that of the 2002 event. This result was consistent with the feature of the observed waveform amplitudes shown in Fig. 1. The rupture of SMGA1 propagated in the down-dip direction, whereas the rupture of SMGA2 propagated northeastward in the up-dip direction. The result reflects the difference in the pulse width and amplitude of the displacement waveforms between SMGA1 and SMGA2.

Kubo et al.[21] and Sakoda et al.[22] analyzed the kinematic source process of this earthquake by the waveform inversion method using low-frequency components of observed strong motion waveforms. Their results indicated large slips in two locations on the source fault; one was in the vicinity of the hypocenter and the other one was located to the southeast of the hypocenter. Figure 5 shows two SMGAs estimated in this study and the slip distribution by Kubo et al.[21] overlaid on the same map. Kubo et al.[21] analyzed the kinematic source rupture process using the velocity waveforms in the frequency range 0.1–1 Hz recorded at 18 strong motion stations of NIED K-NET, KiK-net and F-net. They used station-dependent one-dimensional velocity structure models for computing the theoretical Green's functions for each station. The location and spatial extent of the two SMGAs corresponded to the large slip region estimated by the waveform inversion analysis using the lower frequency waveforms (< 1 Hz). The rupture time of the large slip located to the southeast of the hypocenter was estimated to be 2.4–4.8s after the origin time in Kubo et al.[21], and it was consistent with the rupture time and rise time of SMGA2 in this study. Therefore, it was confirmed that the large slip region (asperity) and SMGAs corresponded to each other spatially and temporally for this earthquake. The spatio-temporal correlation between large slip and SMGA was also reported for the 2005 off-Miyagi earthquake ($M_{JMA}$ 7.2)[23], but further knowledge regarding this point needs to be accumulated in the future. Sakoda et al.[22] also analyzed the 2002 event using the kinematic waveform inversion method, and found that the source time function of the rupture in the vicinity of the hypocenter of the 2015 event is similar to the source time function of the 2002 event. They pointed out that a similar rupture process was progressing in the initial stage of the rupture, although the magnitudes of the earthquakes differed between the two events.

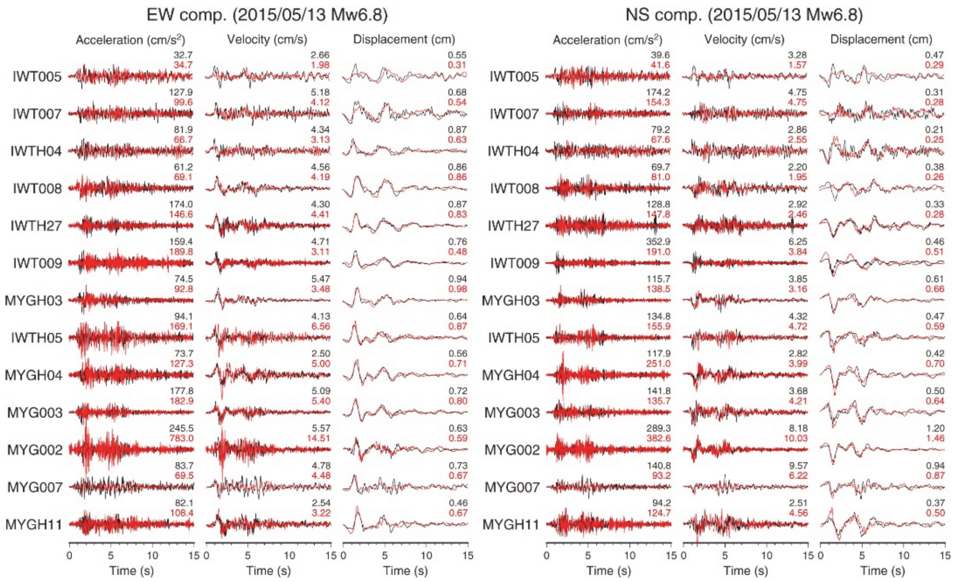


Fig. 4 Observed (black) and synthetic (red) waveforms of the 2015 Kesennuma earthquake. The value above each trace represents the maximum amplitude.

Table 3 SMGA source parameters of the 2015 off-Kesennuma earthquake

| | Parameters | | Search range | Search interval | Results |
|---|---|---|---|---|---|
| Common | Strike / Dip / Rake | | Referring to NIED F-net MT | | 178° / 25° / 64° |
| Common | Rupture velocity within SMGA | | 2.4–4.0 km/s | 0.2 km/s | 3.0 km/s |
| SMGA1 | $N$ | | Determined by trial-and-error | | 5 |
| SMGA1 | $C$ | | 2.0–4.0 | 0.1 | 3.9 |
| SMGA1 | Length $L$ | | $L = N \cdot l$ | | 5.5 km |
| SMGA1 | Rise time $T$ | | $T = N \cdot \tau$ | | 1.9 s |
| SMGA1 | Rupture starting point in SMGA | Along strike | 1–5 | 1 | 3 |
| SMGA1 | Rupture starting point in SMGA | Along dip | 1–5 | 1 | 2 |
| SMGA1 | Seismic moment $M_0$ | | $M_0 = CN^3 \cdot m_0$ | | $6.39 \times 10^{18}$ Nm |
| SMGA1 | Stress drop $\Delta\sigma$ | | Circular crack model[17] | | 93.5 MPa |
| SMGA2 | Rupture starting point relative to the hypocenter | Along strike | 4.0–8.0 km | 1.0 km | 7.0 km |
| SMGA2 | Rupture starting point relative to the hypocenter | Along dip | −6.0–0.0 km | 1.0 km | −3.0 km |
| SMGA2 | Rupture time relative to SMGA1 | | 2.0–3.0 s | 0.1 s | 2.2 s |
| SMGA2 | $N$ | | Determined by trial-and-error | | 5 |
| SMGA2 | $C$ | | 2.0–4.0 | 0.1 | 3.4 |
| SMGA2 | Length $L$ | | $L = N \cdot l$ | | 5.5 km |
| SMGA2 | Rise time $T$ | | $T = N \cdot \tau$ | | 1.9 s |
| SMGA2 | Rupture starting point in SMGA | Along strike | 1–5 | 1 | 5 |
| SMGA2 | Rupture starting point in SMGA | Along dip | 1–5 | 1 | 5 |
| SMGA2 | Seismic moment $M_0$ | | $M_0 = CN^3 \cdot m_0$ | | $5.57 \times 10^{18}$ Nm |
| SMGA2 | Stress drop $\Delta\sigma$ | | Circular crack model[17] | | 81.5 MPa |

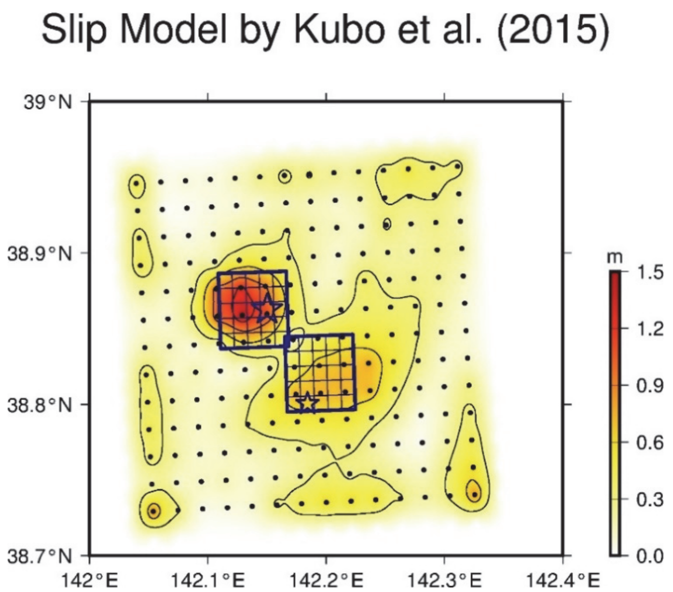


Fig. 5 Comparison of SMGAs of the 2015 off-Kesennuma earthquake with the slip model by Kubo et al.[21]. Large star: hypocenter located by JMA, small star: rupture starting point of SMGA2.

## 4. STRONG MOTION WAVEFORM MODELING AT THE OFUNATO-BOCHI STATION

### 4.1 The 2002 and 2015 off-Kesennuma earthquakes

The strong ground motions were simulated at OFN using the source models of the 2002 and 2015 events obtained in the preceding section. However, since the strong motion record of the small event on November 4, 2002 was not available at OFN, the waveform record observed at K-NET IWT008 (Ofunato station), which is close to Ofunato Port, was used as an EGF. The surface geology[24] is slate rock of upper Permian Toyoma Formation at IWT008, and it is slate rock of lower Cretaceous Ofunato Group at OFN. Thus, both can be regarded as outcrop rock. Moreover, Nozu and Wakai[25] reported that both have no obvious amplification based on the empirical site amplification factors and microtremor H/V spectra measured at these two sites. For the above reasons, the waveform record of the small event observed at IWT008 was used as the EGF for OFN by correcting only the difference in the hypocentral distance.

Figure 6 shows the observed and synthetic acceleration, velocity, and displacement waveforms at OFN. In this figure, 02OFN and 15OFN represent the 2002 event and the 2015 event, respectively. All the observed waveform data were processed records equivalent to the SMAC-B2 type accelerograph, and the EGF record was convolved with the instrument response of SMAC-B2. The bandpass filter in the frequency range from 0.4 to 4 Hz was applied to both observed and synthetic waveforms. The waveform characteristics of the S-wave portion and its duration were well reproduced for both events.

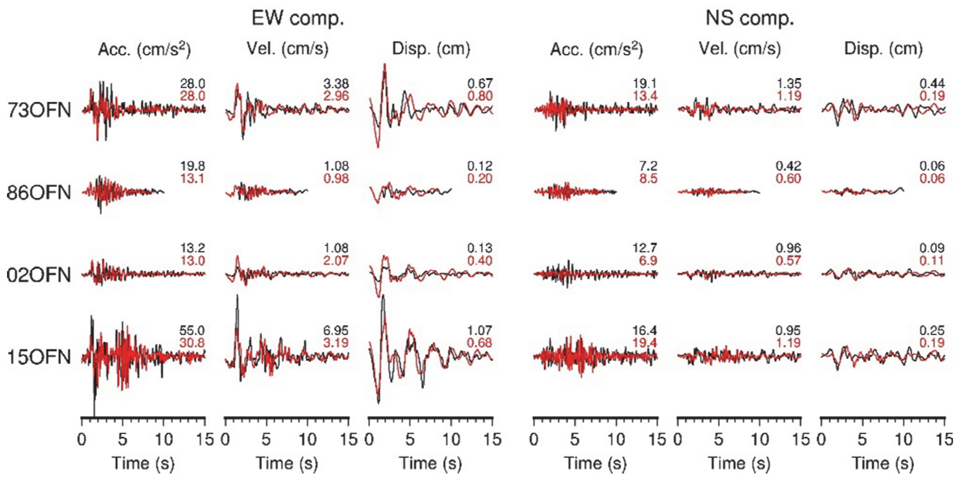


Fig. 6 Observed (black) and synthetic (red) waveforms at OFN for the 1973, 1986, 2002, and 2015 off-Kesennuma earthquakes. The value above each trace represents the maximum amplitude.

### 4.2 The 1973 and 1986 off-Kesennuma earthquakes

The SMGA source models were estimated for the 1973 and 1986 events by waveform modeling of the two horizontal components at OFN. The EGF event and its source parameters (spatial size and rise time) were the same as the 2002 event. The unknown model parameters for grid search were the *C* factor, rupture propagation velocity, and rupture starting sub-fault in the SMGA. Table 4 summarizes the estimated source models, and comparison between the observed and synthetic waveforms were shown together in Fig. 6. The SMGA of the 1973 event ruptured propagating mainly in the down-dip direction, and the rupture propagation direction and rupture propagation velocity were similar to the SMGA of the 2002 event and the SMGA1 of the 2015 event. On the other hand, the best solution for the 1986 event indicated that the rupture propagation direction of the SMGA was the up-dip direction and its rupture propagation velocity was 3.8 km/s, which was faster than the other three events. From OFN, the rupture progressed in the backward direction, so it is thought that the fast rupture propagation velocity resulted in the same pulse width in the velocity and displacement waveforms as in the other earthquakes. When the rupture propagation velocity was fixed at 3.0 km/s in the grid search, the rupture starting sub-fault number was estimated to be (4,1), which corresponded to the rupture propagation in the down-dip direction, but the residual was larger than the above mentioned best solution. Since this analysis used only the records at one location, it might be less reliable than the analysis of the 2002 and 2015 events, and it was difficult to discuss the detailed rupture direction. However, the amount of stress drop was consistent with the simple comparison of observed waveforms (Fig. 1), and we believe that a reasonable result was obtained within the limitation of data.

Table 4 SMGA source parameters of the 1973 and 1986 off-Kesennuma earthquakes

| | Parameters | | Search range | Search interval | Results |
|---|---|---|---|---|---|
| SMGA of the 1986 event | Strike / Dip / Rake | | Referring to Global CMT project [26] | | 187° / 23° / 75° |
| | $N$ | | Determined by trial-and-error | | 5 |
| | $C$ | | 2.0–5.0 | 0.1 | 2.4 |
| | Lentgh $L$ | | $L = N \cdot l$ | | 5.5 km |
| | Rise time $T$ | | $T = N \cdot \tau$ | | 1.9 s |
| | Rupture velocity | | 2.4–4.0 km/s | 0.2 km/s | 3.8 km/s |
| | Rupture starting point in SMGA | Along strike | 1–5 | 1 | 3 |
| | | Along dip | 1–5 | 1 | 5 |
| | Seismic moment $M_0$ | | $M_0 = CN^3 \cdot m_0$ | | $3.93 \times 10^{18}$ Nm |
| | Stress drop $\Delta\sigma$ | | Circular crack model [17] | | 57.5 MPa |
| SMGA of the 1973 event | Strike / Dip / Rake | | Referring to Kao and Chen (1996) [27] | | 174° / 23° / 62° |
| | $N$ | | Determined by trial-and-error | | 5 |
| | $C$ | | 2.0–5.0 | 0.1 | 3.7 |
| | Lentgh $L$ | | $L = N \cdot l$ | | 5.5 km |
| | Rise time $T$ | | $T = N \cdot \tau$ | | 1.9 s |
| | Rupture velocity | | 2.4–4.0 km/s | 0.2 km/s | 3.0 km/s |
| | Rupture starting point in SMGA | Along strike | 1–5 | 1 | 4 |
| | | Along dip | 1–5 | 1 | 2 |
| | Seismic moment $M_0$ | | $M_0 = CN^3 \cdot m_0$ | | $6.06 \times 10^{18}$ Nm |
| | Stress drop $\Delta\sigma$ | | Circular crack model [17] | | 88.7 MPa |

## 5. DISCUSSIONS

The SMGA source models of the four events analyzed in this study are plotted together on the map in Fig. 7. These SMGAs overlap spatially except SMGA2 of the 2015 event. The figure also shows the horizontal error of the hypocenter location in the JMA unified earthquake catalog. As is clear from this figure, since the distribution of seismic stations used for hypocenter locating is biased toward the land area of the Tohoku region, which is long in the north and south, the location error in the longitude direction tends to be larger than in the latitude direction. Especially in the case of old earthquakes before 1973, the error of the hypocenter location in the longitudinal direction is about 6–8 km. In the analyses of this study, the rupture starting point was fixed at the hypocenter in the JMA unified earthquake catalog. Hence, if we consider the horizontal error of the hypocenter location, it can be concluded that there is a high possibility that the SMGA1 of the 2015 off-Kesennuma earthquake ruptured repeatedly in the 1973, 1986, and 2002 off-Kesennuma earthquakes. If the physical entity of the SMGA is defined by the inhomogeneity of the plate boundary surface, it can be considered that it does not change in space significantly in a short period of geological time. Of course, the results can not completely exclude the possibility that there are non-overlapping ones in the last four times. However, the *M*6-class aftershocks of the 2011 Tohoku earthquake, which occurred three times in a short time on the west (near 38° 52' N, 142° 05' E) of the source region of the off-Kesennuma repeating earthquakes studied in this study, have different waveform characteristics than the off-Kesennuma repeating earthquakes[13), 22)]. This fact means that the source process and the Green's functions are different between the adjacent groups of earthquakes, and it could be concluded that there is a high relevance between the differences in the source location and the observed strong motion waveforms. Since it is not clear at present what kind of physical and geological conditions cause the SMGA, therefore, whether the SMGA is conserved in space or not depends on the one's view of the earthquake. Even if they do not completely overlap, the purpose of this paper and engineering significance of discussing variations in the source characteristics of plate boundary earthquakes that repeatedly occur in the same source region do not change.

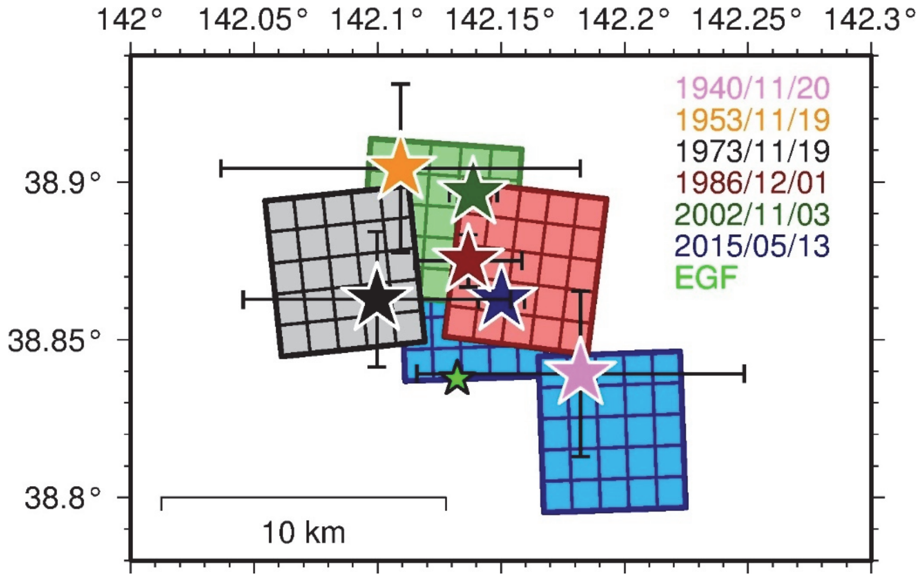


Fig. 7 Epicenters and SMGAs of the repeating plate-boundary earthquakes occurring offshore of Kesennuma, northeast Japan.

The stress drop in SMGAs for the last four off-Kesennuma earthquakes was estimated in the range of 57.5 MPa to 93.5 MPa, and the difference between the smallest and largest events was 1.6 times. This estimate was close to the result of 1.5 times obtained in the previous work[9)] for the 1982 and 2008 off-Ibaraki earthquakes. Based on the results of the two source regions in northeastern Japan, the estimated stress drop in SMGA for the repeating earthquake occurring in the same source region has fluctuations of 1.5–1.6. The average of the stress drops in five SMGAs for the last four off-Kesennuma earthquakes was 76.2 MPa, and all the results fell in the range of 0.75 to 1.2 times of the average. These findings can be useful knowledge for reasonably giving the variation or uncertainty to the source parameters of SMGA when we set up a source model for the strong motion prediction. Moreover, no clear relationship was found between the stress drop (i.e., slip) and the earthquake occurrence interval for the last four events.

Tomita et al.[28)] reported that the displacement rate of the Pacific Plate near the Japan Trench after the 2011 Tohoku earthquake was 18.0 ± 4.5 cm/yr relative to the North American Plate by directly measuring using a GPS/acoustic technique. It was almost twice as fast as the predicted interseismic plate motion based on the MORVEL model[29)], and they concluded that the obtained incoming plate displacement rate could be explained by the sum of the viscoelastic relaxation and steady plate motion. Such significant change in the surrounding tectonic setting might be related to the fact that the magnitude and stress drop, or slip, of the 2015 off-Kesennuma earthquake were large. Although the 1940 event could not be analyzed in this study, the epicenter plotted in Fig. 7 was located slightly to southeast of other earthquakes, and its $M_{\mathrm{JMA}}$ was 6.6, which was relatively large. From the above information, it might be possible to have speculation that that both SMGA1 and SMGA2 were involved during the 1940 event, as in the case of the 2015 earthquake, or that the 1940 event had a somewhat different source process from the last four earthquakes.

## 6. CONCLUSIONS

In this study, strong motion waveform modeling was performed using the empirical Green's function method for four M6-class earthquakes occurring repeatedly with an average recurrence interval of about 15 years on the plate boundary off Kesennuma, northeast Japan. The results showed that the 2002 event had one SMGA, and the 2015 event had two SMGAs. The strong motion waveform modeling of the 1973, 1986, 2002, and 2015 events was also performed at the Ofunato-bochi strong motion station (OFN), where strong motion observation had continued at the same location for over 50 years. The SMGAs of these four repeating earthquakes were located at almost the same location, but the stress drop varies between 57.5 MPa and 93.5 MPa. Considering together with the past study for off Ibaraki earthquakes, the SMGA of the plate boundary earthquakes occurring in the same source region in northeast Japan has fluctuation of about 1.5 to 1.6 times in its stress drop relative to the smallest event or ± 25% of the average stress drop. It goes without saying that there are still a limited number of analyzed cases, but it is clear that the uncertainty or variation in the stress drop amount in the SMGA should be appropriately considered in setting of the source parameters for the strong motion prediction for earthquakes in these regions.

It is essential to continue strong motion observations for analyzing repeating earthquakes in the same source region and examining the difference in the source characteristics as done in this study. Since the recurrence interval is short for M6-class earthquakes on the plate-boundary interface off Kesennuma, the last two events have been recorded at a large number of strong motion stations belonging to K-NET and KiK-net of NIED. Moreover, four earthquakes in the same source region could be successfully analyzed in the same way by using the records from the Strong-Motion Earthquake Observation Network in Japanese Ports. It is expected that valuable strong motion records will be accumulated and released in the future, and that basic research contributing to the enhancement of the strong motion prediction and earthquake hazard assessment will be carried out.

## ACKNOWLEDGMENT

The strong motion data were provided from the Strong-Motion Earthquake Observation Network in Japanese Ports[10)] and NIED[30)]. The JMA unified hypocenter catalog was published as the Seismological Bulletin of Japan by JMA in collaboration with the Ministry of Education, Culture, Sports, Science, and Technology (MEXT). This study also referred to moment tensor catalogs by the NIED F-net project and the Global centroid-moment-tensor (CMT) project. The presentation materials for the 2002 off-Kesennuma earthquake authored by Dr. Wataru Suzuki was helpful for starting this study. This study was financially supported by Grant-in-Aid for Young Scientists (B) of the Japan Society for Promotion of Science (JSPS) 25750146, Grant-in-Aid for Scientific Research (B) of JSPS 26282104, the Kyoto University Foundation, and Earthquake and Volcano Hazards Observation and Research Program of MEXT. All figures were drawn using the Generic Mapping Tools v. 5.4[31)]. Discussions during the 15th Japan Earthquake Engineering Symposium were fruitful for preparing this paper. The author also sincerely appreciated two anonymous reviewers and editors for comments to improve the original manuscript.

## REFERENCES


1) Maeda, T., Iwaki, A., Morikawa, N., Aoi, S. and Fujiwara, H.: Seismic-Hazard Analysis of Long-Period Ground Motion of Megathrust Earthquakes in the Nankai Trough Based on 3D Finite-Difference Simulation, *Seismological Research Letters*, Vol. 87, No. 6, pp. 1265–1273, 2016.
2) Irikura, K. and Miyake, H.: Recipe for Predicting Strong Ground Motion from Crustal Earthquake Scenarios, *Pure and Applied Geophysics*, Vol. 168, Nos. 1–2, pp. 85–104, 2011.
3) Headquarters for Earthquake Research Promotion: Strong ground motion prediction method for earthquakes with specified source faults ("Recipe") (Updated version on April 27, 2017), 2017. https://www.jishin.go.jp/main/chousa/17_yosokuchizu/recipe.pdf. (in Japanese, last accessed on July 3, 2020)
4) Murotani, S., Miyake, H. and Koketsu, K.: Scaling of characterized slip models for plate-boundary earthquakes, *Earth, Planets and Space*, Vol. 60, No. 9, pp. 987–991, 2008.
5) Allmann, B. P. and Shearer, P. M.: Global variations of stress drop for moderate to large earthquakes, *Journal of Geophysical Research*, Vol. 114, No. B1, B01310, doi:10.1029/2008JB005821, 2009.
6) Somei, K., Asano, K., Iwata, T. and Miyakoshi, K.: Source Scaling of Inland Crustal Earthquake Sequences in Japan Using the S-Wave Coda Spectral Ratio Method, *Pure and Applied Geophysics*, Vol. 171, No. 10, pp. 2747–2766, 2014.
7) Nagai, R., Kikuchi, M. and Yamanaka, Y.: Comparative Study on the Source Processes of Recurrent Large Earthquakes in Sanriku-oki Region: The 1968 Tokachi-oki Earthquake and the 1994 Sanriku-oki Earthquake, *Zisin (Journal of Seismological Society of Japan) 2nd Series*, Vol. 54, No. 2, pp. 267–280, 2001. (in Japanese with English abstract)
8) Yamanaka, Y. and Kikuchi, M.: Asperity map along the subduction zone in northeastern Japan inferred from regional seismic data, *Journal of Geophysical Research*, Vol. 109, No. B7, B07307, doi:10.1029/2003JB002683, 2004.
9) Takiguchi, M., Asano, K. and Iwata, T.: The Comparison of Source Models of Repeating Subduction-zone Earthquakes Estimated Using Broadband Strong Motion Records −1982 and 2008 Ibaraki-ken-oki M7 Earthquakes−, *Zisin (Journal of Seismological Society of Japan) 2nd Series*, Vol. 63, No. 4, pp. 223–242, 2011. (in Japanese with English abstract)
10) Nozu, A. and Nagasaka, Y.: Annual Report on Strong-Motion Earthquake Records in Japanese Ports (2015), *Technical Note of the Port and Airport Research Institute*, No. 1331, 24 p., 2017. (in Japanese)
11) Irikura, K.: Prediction of strong acceleration motions using empirical Green's function, *Proceedings of the 7th Japan Earthquake Engineering Symposium*, pp. 151–156, 1986.
12) Hasegawa, Y., Hashimoto, T., Kusano, F., Yoshikawa, K. and Onishi, S.: Detection of the Characteristic Earthquake Activity of the Middle Class Earthquakes in the Tohoku District, Japan, *Zisin (Journal of Seismological Society of Japan) 2nd Series*, Vol. 58, No. 1, pp. 67–70, 2005. (in Japanese with English abstract)
13) Takasai, Y., Shimokawa, J., Hasegawa, Y., Ohta, K., Tamaribuchi, K. and Kusano, F.: Survey of Moderate Repeating Earthquakes in the Tohoku District, *Technical Reports of the Meteorological Research Institute*, No. 72, pp. 85–107, 2014. (in Japanese)
14) Ichii, K., Sato, Y., Sato, Y., Hoshino, Y. and Iai S.: Site Characteristics of Strong Motion Earthquake Stations in Ports and Harbours in Japan (Part VI), *Technical Note of the Port and Harbour Research Institute, Ministry of Transport, Japan*, No. 935, 696 p., 1999.
15) Suzuki, W. and Iwata, T.: Source Model of the 2002 Miyagi-Oki Interplate Earthquake ($M_W = 6.4$) Obtained by Strong Ground Motion Simulation Using Empirical Green's Function Method, *Abstracts of American Geophysical Union 2003 Fall Meeting*, S52A-0115, 2003.
16) Miyake, H., Iwata, T. and Irikura, K.: Source Characterization for Broadband Ground-Motion Simulation: Kinematic Heterogeneous Source Model and Strong Motion Generation Area, *Bulletin of the Seismological Society of America*, Vol. 93, No. 6, pp. 2531–2545, 2003.
17) Eshelby, J. D.: The determination of the elastic field of an ellipsoidal inclusion, and related problems, *Proceedings of the Royal Society of London, Series A*, Vol. 241, pp. 376–396, 1957.

18) Satoh, T., Kawase, H. and Sato, T.: Statistical Spectral Model of Earthquakes in the Eastern Tohoku District, Japan, Based on the Surface and Borehole Records Observed in Sendai, *Bulletin of the Seismological Society of America*, Vol. 87, No. 2, pp. 446–462, 1997.
19) Asano, K. and Iwata, T.: Source model for strong ground motion in 0.1–10 Hz during the 2011 Tohoku earthquake, Earth, Planets and Space, Vol. 64, No. 12, pp. 1111–1123, 2012.
20) Miyake, H., Iwata, T. and Irikura, K.: Strong Ground Motion Simulation and Source Modeling of the Kagoshima-ken Hokuseibu Earthquakes of March 26 ($M_{\mathrm{JMA}}$ 6.5) and May 13 ($M_{\mathrm{JMA}}$ 6.3), 1997, Using Empirical Green's Function Method, *Zisin (Journal of Seismological Society of Japan) 2nd Series*, Vol. 51, No. 4, pp. 431–442, 1999. (in Japanese with English abstract)
21) Kubo, H., Kimura, T., Suzuki, W., Aoi, S. and Sekiguchi, H.: Rupture process of the 2015 Miyagi-oki earthquake derived from near-source strong-motion records, *Report of the Coordinating Committee for Earthquake Prediction, Japan*, Vol. 94, pp. 64–70, 2015. (in Japanese)
22) Sakoda, K., Tanaka, M. and Ueda, M.: Source Process of Recurrent Earthquakes Off Kesennuma, Miyagi Prefecture, *Programme and Abstracts, the Seismological Society of Japan, Fall Meeting*, S08-P07, 2015. (in Japanese)
23) Suzuki, W. and Iwata, T.: Source model of the 2005 Miyagi-Oki, Japan, earthquake estimated from broadband strong motions, *Earth, Planets and Space*, Vol. 59, No. 11, pp. 1155–1171, 2007.
24) Takeuchi, M., Kano, K., Ujiie-Mikoshiba, M., Nakagawa, M. and Komazawa M.: *Geological Map of Japan 1:200,000, Ichinoseki*, Geological Survey of Japan, AIST, 2005.
25) Nozu, A. and Wakai, A.: Investigation of Site Effects at Damaged Ports during the 2011 Great East Japan Earthquake Disaster, *Journal of Japan Society of Civil Engineers, Series A1 (Structural Engineering & Earthquake Engineering)*, Vol. 68, No. 4, pp. I_169–I_185, 2012. (in Japanese with English abstract)
26) Dziewonski, A. M., Ekström, G., Woodhouse, J. H. and Zwart, G.: Centroid-moment tensor solutions for October–December 1986, *Physics of Earth and Planetary Interiors*, Vol. 48, Nos. 1–2, pp. 5–17, 1987.
27) Kao, H. and Chen, W.-P.: Seismicity in the outer rise-forearc region and configuration of the subducting lithosphere with special reference to the Japan Trench, *Journal of Geophysical Research*, Vol. 101, No. B12, pp. 27811–27831, 1996.
28) Tomita, F., Kido, M., Osada, Y., Hino, R., Ohta, Y. and Iinuma, T.: First measurement of the displacement rate of the Pacific Plate near the Japan Trench after the 2011 Tohoku-Oki earthquake using GPS/acoustic technique, *Geophysical Research Letters*, Vol. 42, No. 20, pp. 8391–8397, 2015.
29) DeMets, C., Gordon, R. G. and Argus, D. F.: Geologically current plate motions, *Geophysical Journal International*, Vol. 181, No. 1, pp. 1–80, 2010.
30) National Research Institute for Earth Science and Disaster Resilience: NIED K-NET, KiK-net, National Research Institute for Earth Science and Disaster Resilience, doi:10.17598/NIED.0004, 2019.
31) Wessel, P., Smith, W. H. F., Scharroo, R., Luis, J. and Wobbe, F.: Generic Mapping Tools: Improved version released, *Eos, Transactions, American Geophysical Union*, Vol. 94, No. 45, pp. 409–410, 2013.

**(Original Japanese Paper Published: September, 2019)**
**(English Version Submitted: May 25, 2020)**
**(English Version Accepted: July 3, 2020)**